Journal of Molecular Structure 1274 (2023) 134484

Contents lists available at ScienceDirect

Journal of Molecular Structure

journal homepage: www.elsevier.com/locate/molstr

Effect of heteroatoms on structural, electronic and spectroscopic properties of polyfuran, polythiophene and polypyrrole: A hybrid DFT approach

Asma Hassan[a], Muhammad Ismail[a], Ali H. Reshak[b,c,d,*], Zeshan Zada[e], Abdul Ahad Khan[f], Fazal Ur Rehman M[g], Muhammad Arif[h], Khadija Siraj[a], Shafqat Zada[i], G. Murtaza[j,k], Muhammad M. Ramli[c]

[a] Department of Chemistry, Women University Swabi, Swabi 23430, KP, Pakistan
[b] Physics Department, College of Science, University of Basrah, Basrah 61004, Iraq
[c] Center of Excellence Geopolymer and Green Technology (CEGeoGTech), University Malaysia Perlis, 01007 Kangar, Perlis, Malaysia
[d] Department of Instrumentation and Control Engineering, Faculty of Mechanical Engineering, CTU in Prague, Technicka 4, 616607 Prague, Czechia
[e] Beijing National Laboratory for Condensed Matter Physics, Institute of Physics, Chinese Academy of Sciences, Beijing 100190, China
[f] Department of Physics, University of Peshawar, KP, Pakistan
[g] Department of Chemistry, Lahore Garrison University, Pakistan
[h] Department of Physics, Abdul Wali Khan University, Mardan, Pakistan
[i] Department of bioChemistry, Quaid e azam University of Islamabad, Pakistan
[j] Materials Modelling Lab, Department of Physics, Islamia College University, Peshawar, Pakistan
[k] Department of Mathematics & Natural sciences, Prince Mohammad Bin Fahd University, P. O. Box 1664, Alkhobar 31952, Saudi Arabia

ARTICLE INFO

Article history:
Received 18 August 2022
Revised 30 October 2022
Accepted 2 November 2022
Available online 3 November 2022

Keywords:
Heteroatoms
Spectroscopic
Polyfuran
Polythiophene
Polypyrrole
Hybrid DFT Approach

ABSTRACT

In the present manuscript a brief discussion about the new generation of plastic or polymer also called materials of 21st century was conducted. A comparative study of the structural, electronic and spectroscopic properties of the three heterocyclic polymers polypyrrole, polythiophene and polyfuran in neutral form of particular interest has been carried out using the result of Density Function Theory B3LYP/6-31G (d, p) methods. Also how theoretical methods utilizing quantum chemical calculations can be employed to study various properties of these new generation polymers and what information's can be drawn from them about their structural and electronic properties has been discussed. Our major concern is to study the effect of heteroatom i-e O, N, S on electronic, structural and spectroscopic properties of Furans, Pyrrole and Thiophenes. For this purpose, the important structural properties (geometric parameters, charge analysis) spectroscopic properties (vibrational and VU–vis spectra's) and electronic properties (HOMO, LUMO and band gap) of these polymers are compared. The calculated trend in the values of different properties (electronic, structural and spectroscopic) of the polymers is an excellence agreement with available experimental values. The theoretical calculation predicted the order of more attraction as polythiophene (PTh) > polyfuran (PF) > polypyrrole (PPy) from optimized geometric parameters, the Spectroscopic study predict that the λ_{max} absorption shown in the order of PTh > PF > PPy, the HOMO, LUMO and band gap calculation also go side by side with the result obtained from structural and spectroscopic properties calculation

1. Introduction

1.2. Conducting polymers

For long time, polymers were used as insulating materials and considered that polymers do not conduct electricity but more than a Decade now that certain classes of polymers which show conjugation (posses' ∏ conjugation along the polymers backbone) behave like a semiconductor. The presence of delocalization of ∏

* Corresponding author at: Department of Instrumentation and Control Engineering, Faculty of Mechanical Engineering, CTU in Prague, Technicka 4, 616607 Prague, Czechia.
E-mail address: maalidph@yahoo.co.uk (A.H. Reshak).

https://doi.org/10.1016/j.molstruc.2022.134484
0022-2860/

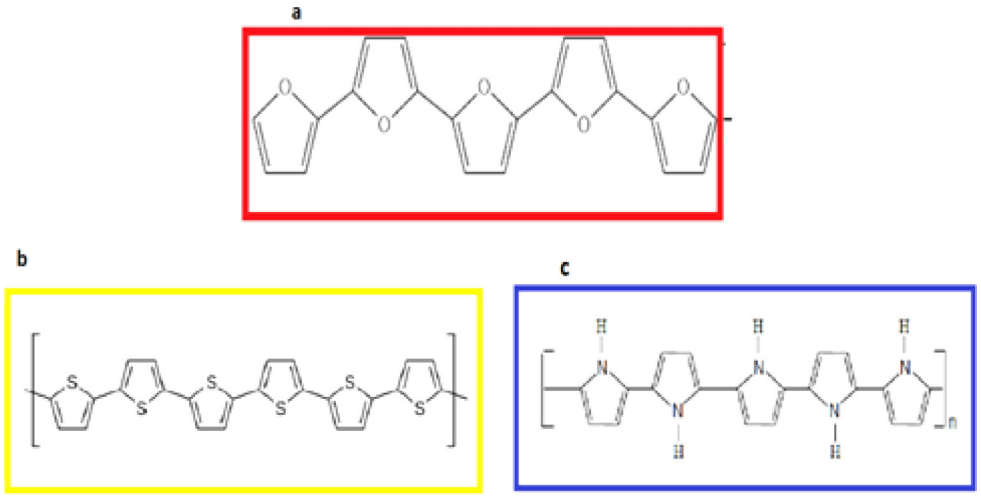

Fig. 1. Chemical structure of PF(a), PTh(b) and PPy(c).

electrons, polymers are able to conduct electricity called conducting polymers. Conduct ing polymers act as substitutes for naturally conductive material [1]. Therefore, the π- electrons play a key role to determine the electrical conductivity and band structure of conducting polymers(2). Conducting polymers have a huge interest in the quest for tough, cheap, flexi ble electronic circuit. Conducting polymers (C.Ps) have many interesting electrical, electrochemical, structural, mechanical and optical properties. Due to their interesting properties C.Ps received a great attention towards its discovery. Discovering C.Ps in the late 1970s by Dr. Hideki Shirakawa, Alan Jay Heega and Graham MacDiarmid at university of Pennsylvania received Nobel prize in 2000 [3]. After discovery of C.Ps scientist found many applications to the newly C.Ps, such as sensor technology, electrochemical devices, super capacitors, construction of Photovoltaic cell, making of re- chargeable batteries, biomedical, artificial nerves etc [4]. Conjugated heterocyclic polymers like (PF), (PPy), (PTh), are very important class of C.Ps [5]. These polymers studied both, theoretically and experimentally have drawn special interest in the field of nanoscience and nanotechnology [6]. Among these C.Ps (PPy) and (PTh) are the most widely studied C.Ps because (PPy) and (PTh) show high conductivity upon doping, chemical stability and nonlinear optical properties [7]. However Polyfuran attracted less attention because polyfuran showed some difficulties in synthesis [7,8]. The Conducting polymers (CPs) have drawn significant interest of researchers for more than 30 years because of their economic importance, superior stability, lighter weight, better workability, resistance to corrosion and satisfactory electrical conductivity. Some applications of CPs are: rechargeable batteries, electro chromic display devices, light reflecting or light transmitting appliances for optical information, sensors and storage for glare reduction systems and smart windows in automobiles and buildings, polymeric light emitting diodes (PLEDs), photovoltaic devices, transistors, electromagnetic shielding against electro-magnetic interferences (EMI) and printed electronic circuits [9]. The chemical structure of PPy, PTh, PF are shown in Fig. 1 below.

Polypyrol is a type of conjugated organic polymers. Among the various C.Ps, PPy have attracted special interest because of their high conductivity [10–12]. PPy has heteroatomic polymers having nitrogen as heteroatom in their five-member ring. The chemical structure of PPy is given in Fig. 1. In 1960 the conjugated organic polymers family received PPY by the pyrolysis of tetraiodopyrol [13]. PPy conduct electricity in the presence of dopant. The conductivity of PPy was exhibited in 1968 [14,15]. Due to some astonishing properties like high flexibility, high conductivity, stabilizes oxidize form, water soluble, superior redox properties, and valuable optical properties, PPy is widely studied C.Ps as both theoretically and experimentally [16]. PPy can be synthesized chemically and electrochemically. Due to the above properties PPy have a large scale of application such as a biosensor, gas sensor [17], actuator, super capacitor etc [18].

PTh is another very interesting conjugated C.Ps [19]. Like PPy, PTh is also a heteroatomic polymer, but in PTh sulfur is the heteroatom in the backbone. PTh is the second generation of C.Ps. The structure of (PTh), as shown in Fig, is linear and conjugated heterocyclic[20]. Like PPy, PTH is very important conjugated polymer due to some properties like storage stability, high electrical conductivity, environmental stability, low weight, good redox ability [21]. PTh has a large scale of applications especially solar cell [22], electrochemical display devices, receptor for detecting chiral molecule etc [23]. PTh results from the polymerization of thiophenes and be- comes conducting when electrons removed or added from the orbital via dopant [24].

Polyfuran is a five member hetetroatomic ring compound having four carbon atoms and one heteroatom (oxygen). Among the heterocyclic polymers such as PPy and PTh, Polyfuran is less studied C.P because it exhibits low conductivity, high oxi dation potential and difficult in synthesis [25]. The structure of PF is analogous to PPy and PTh but the heteroatom (S, NH) is replaced by oxygen in PF. The structure of PF is shown in Fig. 1. PF can be synthesized chemically and electrochemically in organic media. In 1964 PF was synthesized chemically, while synthesizing electrochemically by polymerization of furan has been developed in the past decade. Polyfuran is slightly soluble in water and highly volatile organic compound [26]. PF although has attracted less attention than PPy and PTh but still has many industrial ap plications in insulating form and much technological application in resin form and conversion of solar energy into photo voltaic [27].

2. Computational details

Density function theory (DFT) hybrid function [Becke 3-Parameters (Ex- change), Lee, Yang and parr] B3LYP [28] were employed for the study of geometric, spectroscopic and electronics properties of PPy, PTh and PF. Stimulated all these properties by using split valence basis set (6-31G**). All calculation were carried out by using Gaussian 09 and analyzed the result

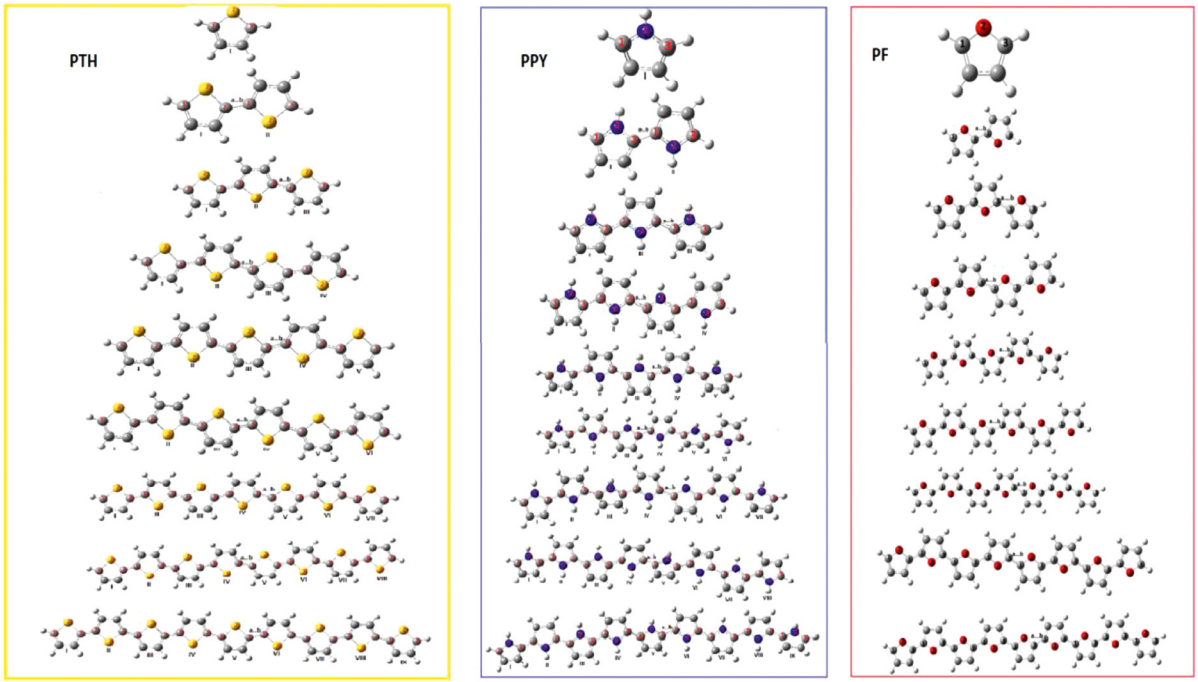

Fig. 2. Optimized bond length of PPy, PF and PTh where n=1...9 repeating units.

by using Gabediet [29] and Gaussian view [30]. nPPy, nPTh and nPF(n=1,2,3,4,5,6,7,8,9) conducting polymers were used (n represent ring number). For geometrical optimization of PPy, PTh, and PF the above mentioned level is used to calculate the parameters (bond angle and bond length). Further simulation such as spectroscopic (UV and IR), Mullikan charge analysis, Natural bond orbital (NBO) analysis, Highest occupied molecular orbital (HOMO), Lowest unoccupied molecular orbital(LUMO) and band gap calculation of PPy, PTh, PF were carried out by using all the above mentioned level of the theory. Optimized geometry and parameters (bond angle and bond length) calculation was obtained by using DFT. Frequencies are assigned by using Gabedet.

The difference between HOMO and LUMO orbital's energy estimates the band gape. The negative of HOMO estimated the ionization potential, while the negative of LUMO is electron affinity. The difference between the HOMO and LUMO energies estimates the electronic properties (natural bond orbital analysis, Mullikan charge analysis) and conductivity measurement (band gape).UV–vis spectra of the PPY,PF and PTH are simulated at DFT using B3LYP basis set 6-31G(d,p) [31]. All the calculations were per- formed by DFT level theory.

3. Results and discussions

3.1. Optimized geometric parameter

Optimization of geometries have been taken as the first task to determine the effect of heteroatom on varies geometric parameters (bond length, bond angle) of the polymers of PF, PPy, and PTh (n=1,...,9 'n' represents number of repeating units). The geometry-optimization was carried out at DFT B3LYP/6-31G** basis set on neutral form. The optimized geometric structures were given in Fig. 2 (bond length), 03 (bond angle) respectively. The optimized geometrical parameters of PF, PPy, PTh are given in Tables 1, 2, 3 (bond length) and Tables 4, 5, 6 (bond angle) respectively. It can be seen from Tables 1, 2, 3 that when the number of ring increases the change in bond length occurs is quit smaller. However, by comparing the optimized geometry of PF, PPy, and PTh it is indicated that the optimized geometry of PF and PPy is in the range of 1.3 and that of PTh is in the range of 1.7 which show that the PF and PPy show small bond alteration with each other while PTh show large bond alteration with PF and PPy in neutral form. According to our theoretically calculated data (Tables 1, 2, 3) the increase in bond length of PF, PPy [32] and PTh is in the or der of PTh > PPy > PF. The intermediate bond length distance from monomer unit to polymer of PPy, PF and PTh have observed to quit same or a very small difference has been observed.

The calculated bond angle of PPy, PF and PTh are totally different from each other as shown in Tables 4, 5, 6. The polymers having large bond length show strong interaction. From bond length calculation we can analyses that the specie having large bond angle has more ability of interaction. As PPy have bond angle in the range of 110°, PF have bond angle in the range of 107°, while PTh have bond length in the range of 91°. The PPy have large bond angle then PF and PTh and thus –NH- site offers strong interaction then PF and PTh. On the basis of our calculated data (Tables 4, 5, 6) the order of strong interaction on the basis of bond PPy > PF > PTh. The intermediate bond angle distance observed from monomer to polymer has been very small. The PPy have intermediate bond distance in the range of 121, PF have 116 and PTh have 120 bond angle intermediate distances. It means that the PF show more interaction due to electronegative –O- heteroatom then –NH- in PPy and –S- in PTh.

3.2. Charge analysis

The charge transferring phenomena for PF, PPy and PTh are simulated by Natural Bonding Orbital (Q_{NBO}) and Mulliken ($Q_{MULLIKEN}$) charge analysis at B3LYP/6-31G (d, p) level of DFT. These properties are basis set dependent; however if the same level of theories is used for different structures [B3LYP/6-31G (d) or B3LYP/6-311++G (d, p)] [35] then the result will provide trend and there for be meaning full. The basis set dependence of these

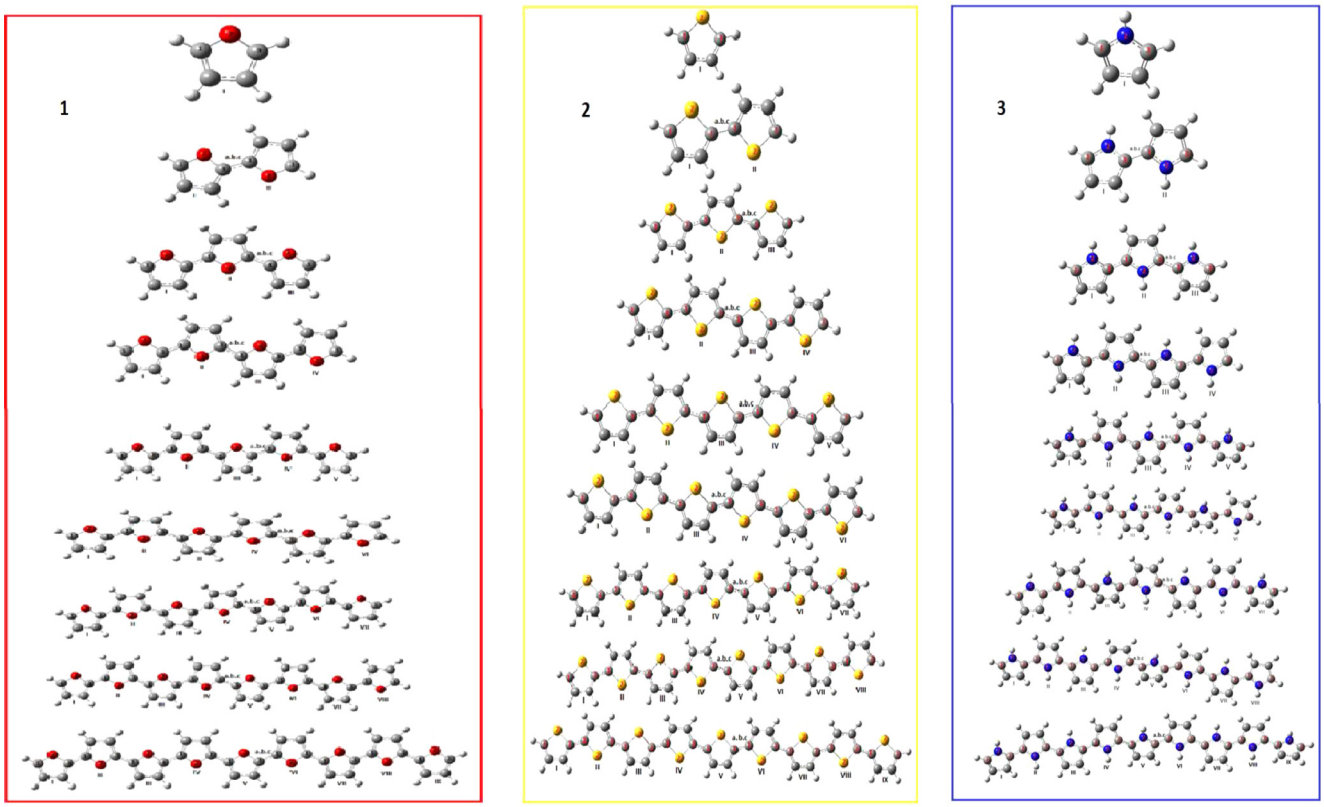

Fig. 3. Optimized bong angle of PF(1), PTh(2) and PPy(3) where n=1...9 repeating units.

charge analysis tool has been discuss by Svantunek et al. [36] and B Han et al. [37].

The net charge distribution for heterocyclic polymers (PF, PTh, PPy) is quite different from each other, as shown in Table 7. The net charge distribution for 1PF is 1.338 based on Mullikan and 2.264 based on NBO, for 1PPy is 1.482 based on Milliken and 2.727 based on NBO while for 1PTh is 1.445 based on Milliken and 2.93 based on NBO. By increasing the conjugated length the net charge distribution of PF, PPy [32], PTh will also increasing. For ring 9 the net charge distribution for PF is 14.21 based on Milliken and 19.37 based on NBO, PPy is 16.838 based on Milliken and 20.882 based on NBO, while PTh is 9.195 based on Mulliken and −18.378 based on NBO. From our theoretical data we conclude that the PTh show minimal net charge distribution from PPy and PF based on Q_{NBO} and $Q_{MULLIKEN}$, while PPy show maximal net charge distribution both in NBO and Milliken. This because the oxygen is the most electro-negative and the Sulphur is the least electronegative of the three heteroatoms.

3.3. UV–vis spectroscopic study

In UV–vis spectra the transition energies and oscillator strength are stimulated by using B3LYP/6 31G (d, p) level of DFT method. Calculated excitation energies, oscillator strength and molecular orbital of the first allowed singlet transitions for PPy, PF, PTh (n= 1…9 repeating units) are given in Tables 8, 9, 10.

Three prominent peaks are observed in UV–vis spectra of PTh λ_{max} of which are observed at 209 nm ($\pi \rightarrow \pi^*$), two prominent peaks are observed in UV–vis spectra of PF and in PPy, the λ_{max} of PF are observed at 190 nm ($\pi \rightarrow \pi^*$) and in PPy λ_{max} observed at 183 nm when n=1. Three prominent peaks are observed in UV–vis spectra of PF, PPy and PTh, λ_{max} of PF are observed at 271 nm, λ_{max} of PTh are observed at 308 nm and λ_{max} of PPy are observed at 254.88 nm when n=2. Three prominent peaks are observed in PTh, λ_{max} are observed at 379.82 nm, four prominent peaks are observed in UV–vis spectra of PF and PPy, λ_{max} of PF are observed at 334.62 nm and that of PPy at 302 nm when n=3. Four prominent peaks are observed in PF, λ_{max} of PF are observed at 383.81 nm, three prominent peaks are observed in PTh and in PPy, λ_{max} of PTh are observed at 437.29 nm and λ_{max} of PPy observed at 341.47 when n=4. Three prominent peaks are observed in PF, λ_{max} of PF observed at 423 nm, two prominent peaks are observed in PPy and in PTh, λ_{max} of PPy observed at 365 nm and in PTh at 482 nm when n=5. Four prominent peaks in UV–vis spectra of PF are ob- served, λ_{max} of PF observed at 454.37 nm, three peaks are observed in UV–vis spectra of PTh and PPy, λ_{max} of PTh observed at 520.67 nm and in PPy at 383.47 nm when n=6. Four peaks in UV–vis spectra of PF are observed, λ_{max} of PF observed at 49.68 nm and three peaks are observed in UV–vis spectra of PPy and PTh, λ_{max} of PPy ob- served at 398.30 nm and PTh at 535.88 nm when n=7. Four prominent peaks are ob- served in UV–vis spectra of PF, λ_{max} of PF observed at 500.18 nm while three peak are observed in UV–vis spectra of PTh and PPy, λ_{max} of PTh observed at 560.42 nm and in PPy at 408.93 nm when n=8. In case of n=9 three prominent peaks are observed in PTh and PPy, λ_{max} of PTh observed at 580.50 nm and in PPy at 417.80 nm, while four prominent peaks are observed in UV–vis spectra of PF, λ_{max} of PF are ob served at 479.68 nm. From the above discussion it is concluded that the different heteroatom's (–O-, -NH- and –S-) in the rings produce comparable spectra as can be seen in the given Fig. 4. The absorption wavelength arising from $S_0 \rightarrow S_1$ electronic transition increases progressively with the increasing of conjugated chain length. Importantly the maximal absorption shows a bathochromic shift when passes from small molecule to big one

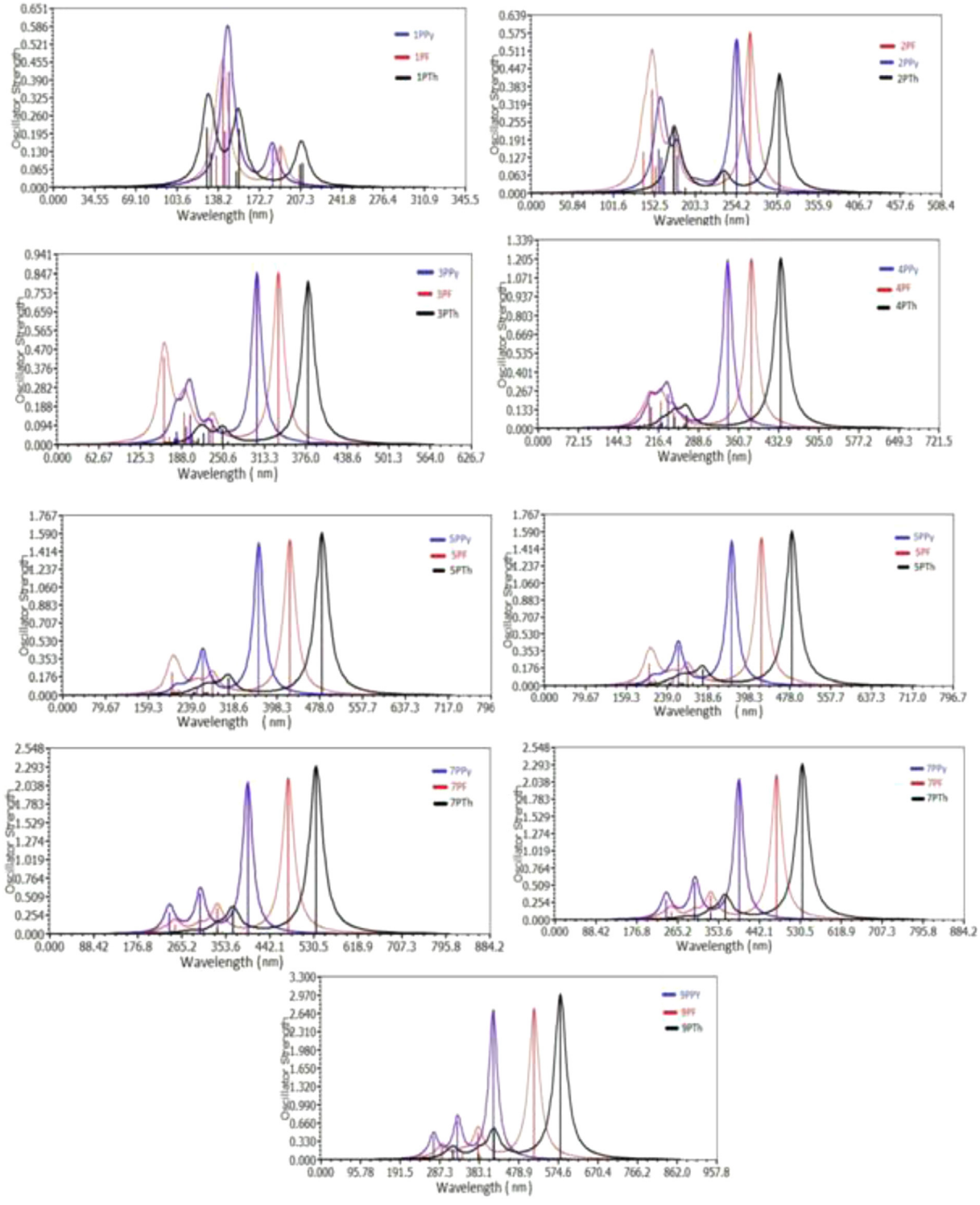

Fig. 4. UV–vis spectrum of PPy, PF, and PTh from n=1...9.

Table 1
(I, II, III): Optimized bond length of polyfuran (n=1, 2, 3, 4, 5, 6, 7, 8, 9), at B3LYP/6-31G (d, p) level of theory. (Atomic labels of Table I, II, III are with reference to Fig. 2.

I: n=1, 2, 3. # of rings with atoms		1PF	2PF	3PF	Exp.
I	1C-2O	1.3642	1.3652	1.36503	1.366
	2O-3C	1.3642	1.3691	1.3697	
II	1C-2O	–	1.3691	1.3706	
	2O-3C	–	1.3652	1.3706	
IV	1C-2O	–	–	1.3697	
	2O-3C	–	–	1.3650	
Intermediate distance (a…b)*		–	1.43847	1.43538	

*:, Intermediate bond distances between rings.
Exp: experimental data from reference [33].

II: n= 4, 5, 6, # of rings with atoms		4PF	5PF	6PF
I	1C-2O	1.3650	1.43538	1.3649
	2O-3C	1.3696	1.3697	1.3696
II	1C-2O	1.3703	1.3702	1.3701
	2O-3C	1.3710	1.3713	1.3712
III	1C-2O	1.3710	1.3710	1.3709
	2O-3C	1.3696	1.3710	1.3711
IV	1C-2O	1.3697	1.3713	1.3711
	2O-3C	1.3651	1.3702	1.3709
V	1C-2O	–	1.3697	1.3712
	2O-3C	–	1.3650	1.3701
VI	1C-2O	–	–	1.3696
	2O-3C	–	–	1.3649
Intermediate distance	(a…b)*	1.43144	1.43090	1.43052

*:, Intermediate bond distances between ring

III: n=7, 8, 9 # of rings with atoms		7PF	8PF	9PF
I	1C-2O	1.36500	1.3650	1.3650
	2O-3C	1.3697	1.3697	1.3697
II	1C-2O	1.3703	1.3702	1.3702
	2O-3C	1.3713	1.3714	1.3714
III	1C-2O	1.3713	1.3709	1.3709
	2O-3C	1.3712	1.3713	1.3713
IV	1C-2O	1.3711	1.3711	1.3711
	2O-3C	1.3711	1.3712	1.3712
V	1C-2O	1.3711	1.3712	1.3711
	2O-3C	1.3709	1.3711	1.3711
VI	1C-2O	1.3714	1.3713	1.3712
	2O-3C	1.3702	1.3709	1.3711
VII	1C-2O	1.3697	1.3713	1.3713
	2O-3C	1.3650	1.3702	1.3709
VIII	1C-2O	–	1.3697	1.3713
	2O-3C	–	1.3650	1.3702
IX	1C-2O	–	–	1.3697
	2O-3C	–	–	1.3650
Intermediate distance (a…b)*		1.43024	1.43010	1.4301

*:, Intermediate bond distances between rings.

Table 2
(I, II, III): Optimized bond length of polypyrrole (n=1, 2, 3, 4, 5, 6, 7, 8, 9), using B3LYP/6-31G(d, p) level of theory. (Atomic labels are with reference to Fig. 2).

I: n=1, 2, 3 # of rings with atoms		1PPy	2PPy	3PPy	Exp.
I	1C-2NH	1.3752	1.3747	1.3745	1.380
	2NH-3C	1.3752	1.3795	1.3801	
II	1C-2NH	–	1.3795	1.3790	
	2NH-3C	–	1.3747	1.3790	
II	1C-2NH	–	–	1.3801	
	2NH-3C	–	–	1.3745	
Intermediate distance (a…b)*		–	1.4494	1.44747	

*: Intermediate bond distances between rings. Exp: experimental data from reference 47.

II: n=4, 5, 6. # of rings with atoms		4PPy	5PPy	6PPy
I	1C-2NH	1.3745	1.3744	1.3744
	2NH-3C	1.3801	1.3802	1.3801
II	1C-2NH	1.3795	1.3787	1.3795
	2NH-3C	1.3804	1.3797	1.3805
III	1C-2NH	1.3804	1.3795	1.3793
	2NH-3C	1.3797	1.3795	1.3796
IV	1C-2NH	1.3801	1.3797	1.3795
	2NH-3C	1.3751	1.3787	1.3794
V	1C-2NH	–	1.3802	1.3797
	2NH-3C	–	1.3743	1.3786
VI	1C-2NH	–	–	1.3802
	2NH-3C	–	–	1.3743
Intermediate distance (a…b)*		1.44442	1.44434	1.44421

*:, Intermediate bond distances between rings.

III: n=7, 8, 9. # of rings with atoms		7PPy	8PPy	9PPy
I	1C-2NH	1.3744	1.3744	1.3743
	2NH-3C		1.3802	1.3802
		1.38021		
II	1C-2NH	1.3787	1.3787	1.3788
	2NH-3C	1.3796	1.3797	1.3797
III	1C-2NH	1.3804	1.3794	1.3803
	2NH-3C	1.3805	1.3795	1.3806
IV	1C-2NH	1.3794	1.3805	1.3793
	2NH-3C	1.3796	1.3795	1.3795
V	1C-2NH	1.3796	1.3794	1.3805
	2NH-3C	1.3794	1.3796	1.3804
VI	1C-2NH	1.3797	1.3796	1.3795
	2NH-3C	1.3787	1.3794	1.3794
VII	1C-2NH	1.3802	1.3797	1.3796
	2NH-3C	1.3743	1.3787	1.3794
VIII	1C-2NH	–	1.3802	1.3797
	2NH-3C	–	1.3743	1.3786
IX	1C-2NH	–	–	1.3802
	2NH-3C	–	–	1.3744
Intermediate distance (a…b)*		1.44418	1.44396	1.44401

*:, Intermediate bond distances between rings

which also can be seen respectively from monomers of PPy, PF, and PTh to 9 repeated units as can be seen from Table 8. From spectroscopic study of PF, PTh and PPy we conclude that the PTh show maximum absorption as compared to PF and PPy. In view of observed and theoretically calculated UV–vis data it would be found that with increasing conjugation length the order of maximum absorption is PTh > PF > PPy.

3.4. Vibrational spectra

The vibrational spectra of PPy, PF and PTh were calculated by using B3LYP/6-31G (d, p) level of DFT method. The observed major band frequencies of PPy, PF, and PTH along with their relative intensities and probable vibration assignment are presented in Table 11. The theoretically calculated I.R spectra of PPy, PTh, and PF are plotted on Origin Pro 8.5 as shown in Fig. 5. Generalized gradient approximation (GGA) is also an appropriate method for simulating the vibration spectra of a finite and infinite number of atoms. H Ullah et al. [38] reported that GGA can successfully predict the structural and vibrational properties of closed and open-shell systems for oxides of actinide compounds. Furthermore, they correlated the reliability of GGA with CASPT2, which is a highly computationally demanding method. Adjokatse et al. [39] had also systematically studied the dielectric and piezoelectric response of odd-numbered nylons with the help of the DFT method with GGA and found nice correlation of the theoretically simulated vibrational spectrum with that of available experimental data. For conducting polymers, literature reveals that pure GGA and hybrid B3LYP are quite effective at simulating the vibrational

Table 3
(I, II, III): Optimized bond length of polythiophene (n=1, 2, 3, 4, 5, 6, 7, 8, 9), using B3LYP/6-31G (d, p) level of theory. (Atomic labels are with reference to Fig. 2).

I: n=1, 2, 3					
# of rings with atoms		1PTh	2PTh	3PTh	Exp
I	1C-2S	1.7357	1.7360	1.7360	1.752
	2S-3C	1.7357	1.7569	1.7580	
II	1C-2S	–	1.7569	1.7575	
	2S-3C	–	1.7360	1.7575	
IV	1C-2S	–	–	1.7580	
	2S-3C	–	–	1.7580	
Intermediate distance (a–b)*		–	1.45061	1.44657	

*: Intermediate bond distance between rings. Exp: experimental data [34].

II: n=4, 5, 6				
# of rings with atoms		4PTh	5PTh	6PTh
I	1C-2S	1.7356	1.7353	1.7351
	2S-3C	1.7577	1.7581	1.7580
II	1C-2S	1.7573	1.7575	1.7573
	2S-3C	1.7582	1.7588	1.7587
III	1C-2S	1.7582	1.7587	1.7586
	2S-3C	1.7573	1.7587	1.7588
IV	1C-2S	1.7577	1.7588	1.7587
	2S-3C	1.7356	1.7575	1.7586
V	1C-2S	–	1.7581	1.7588
	2S-3C	–	1.7353	1.7573
VI	1C-2S	–	–	1.7580
	2S-3C	–	–	1.7352
Intermediate distance (a…b)*		1.44214	1.44165	1.44092

*:, Intermediate bond distances between rings

III: n=7, 8, 9				
# of rings with atoms		7PTh	8PTh	9PTh
I	1C-2S	1.735	1.735	1.735
	2S-3C	1.7572	1.7572	1.7572
II	1C-2S	1.7564	1.7564	1.7564
	2S-3C	1.7577	1.7577	1.7577
III	1C-2S	1.7578	1.7577	1.7577
	2S-3C	1.7581	1.7582	1.7581
IV	1C-2S	1.7581	1.7581	1.758
	2S-3C	1.7581	1.7582	1.7582
V	1C-2S	1.7581	1.7582	1.7582
	2S-3C	1.7578	1.7581	1.7582
VI	1C-2S	1.7578	1.7582	1.7582
	2S-3C	1.7564	1.7577	1.758
VII	1C-2S	1.7572	1.7577	1.7581
	2S-3C	1.735	1.7564	1.7577
VIII	1C-2S	–	1.7572	1.7577
	2S-3C	–	1.735	1.7564
IX	1C-2S	–	–	1.7572
	2S-3C	–	–	1.735
Intermediate distance (a…b)*		1.44161	1.44135	1.4413

*:, Intermediate bond distances between rings

spectra; however, the latter is more abundantly used in the literature [40].

Vibrational spectroscopy is a key characterization for structural elucidation.

The simulated scaled IR spectrum of 1PPy has major prominent band peak at 461.26 cm^{-1} and has assigned twisting vibration, simulated scaled IR spectrum of 1PF has major prominent band peak at 759.54 cm^{-1} assigned wagging vibration, while simulated scaled IR spectrum of 1PTh has major prominent band peak at 729.6 cm^{-1} as- signed asymmetric stretching and ring deformation. The simulated scaled IR spectrum of 2PPy has major prominent band peak at 489.55 cm^{-1} assigned twisting vibration, the simulated scaled IR spectrum of 2PF has major prominent band peak at 733.75 cm^{-1} and also assigned twisting vibration like 2PPy, while the simulated scaled IR spectrum of 2PTh has major prominent band peak at 681 cm^{-1} and assigned wagging vibration. The 3PPy has major prominent band peak at 768.52 cm^{-1} and assigned wagging vibration, 3PF has major prominent peak at 1042 cm^{-1} and assigned scissoring vibration, while 3PTh has major prominent peak at 696.5 cm^{-1} and assigned twisting vibration. The simulated scaled IR major peak band spectrum of 4PPy as- signed scissoring vibration at 1105.01 cm^{-1}, 4PF assigned wagging vibration at799.36 cm^{-1} while 4PTh assigned wagging and ring deformation at 701.2 cm^{-1}. The simulated scaled IR major peak band spectrum of 5PPy assigned wagging vibration at 785.78 cm^{-1}, 5PF assigned scissoring vibration at 1043.23 cm^{-1} while 5PTh assigned asymmetric stretching at 688.3 cm^{-1}. The major prominent IR peak band simulated for 6PPy at 782.67 cm^{-1} assigned wagging vibration, for 6PF at 810.49 cm^{-1} assigned twisting vibration, for PTh at1547.9 cm^{-1} assigned asymmetric stretching vibration. The major peak band of IR simulated for 7PPy at1562.25 cm^{-1} assigned asymmetric stretching and ring deformation, for 7PF at 810.49 cm^{-1} assigned twisting vibration, for 7PTh at 1572.02 cm^{-1} assigned asymmetric stretching and ring deformation. The simulated scaled IR major peak band for 8PPy at 768.81 cm^{-1} assigned wagging vibration, for 8PF at 1552.63 cm^{-1} assigned asymmetric stretching vibration, for 8PTh at 1555 cm^{-1} also assigned asymmetric stretching vibration. The simulated scaled IR spectrum of 9PPy has major prominent band peak at 762.60 cm^{-1} and assigned wag- ging, simulated scaled IR spectrum of 9PF has major prominent band peak at 1553.53 cm^{-1} assigned asymmetric stretching vibration while simulated scaled IR spectrum of 9PTh has major band peak at 1563.1 cm^{-1} and assigned asymmetric stretching vibration.

3.5. HOMO LUMO energy gap

The HOMO and LUMO energy of polypyrrole (PPy), polyfuran (PF) and polythiophene (PTh) calculated at B3LYP/6-31G (d, p) level of DFT. The HOMO and LUMO energy give information about electronic properties such as ionization potential (I.P), electron affinity (E.A) and energy gap. "range-separated functionals estimates HOMO–LUMO gaps and excited-state energies better" [41–44]. The

Table 4
Optimized bond angle of polythiophene (n=1, 2, 3, 4, 5, 6, 7, 8, 9), using B3LYP/6-31G** level of theory (Atomic labels are with reference to Fig. 3).

Spe- cies	1 1C-2S-3C	II 1C-2S-3C	III 1C-2S-3C	IV 1C-2S-3C	V 1C-2S-3C	VI 1C-2S-3C	VII 1C-2S-3C	VIII 1C-2S-3C	IX 1C-2S-3C	a…b…c*
1PTh	91.51	––	––	––	––	––	––	––	––	––
2PTh	91.83	91.83	––	––	––	––	––	––	––	120.93
3PTh	91.78	92.17	91.79	––	––	––	––	––	––	120.79
4PTh	91.80	92.17	92.17	91.80	––	––	––	––	––	120.85
5PTh	91.77	92.14	92.13	92.15	91.77	––	––	––	––	120.79
6PTh	91.78	92.14	92.12	92.12	92.14	91.78	––	––	––	120.82
7PTh	91.76	92.10	92.09	92.09	92.09	92.10	91.76	––	––	120.78
8PTh	91.75	92.10	92.09	92.09	92.09	92.09	92.10	91.76	––	120.79
9PTh	91.75	92.10	92.09	92.09	92.09	92.09	92.09	92.10	91.76	120.80

*:, an intermediate bond distances between rings.

Table 5
Optimized bond angle (°) of polyfuran (n=1, 2, 3, 4, 5, 6, 7, 8, 9), using B3LYP/6-31G** level of theory (Atomic labels are with reference to Fig. 3).

Spe- cies	I 1C-2O-3C	II 1C-2O-3C	III 1C-2O-3C	IV 1C-2O-3C	V 1C-2O- 3C	VI 1C-2O- 3C	VII 1C-2O-3C	VIII 1C-2O-3C	IX 1C-2O-3C	a....b...c*
1PF	106.77	––	––	––	––	––	––	––	––	––
2PF	106.94	106.94	––	––	––	––	––	––	––	116.68
3PF	106.94	107.09	106.93	––	––	––	––	––	––	116.75
4PF	106.89	107.08	107.08	106.89	––	––	––	––	––	116.72
5PF	106.90	107.07	107.08	107.07	106.9 0	––	––	––	––	116.74
6PF	106.89	107.06	107.068 82	107.06	107.0 6	106.8 9	––	––	––	116.76
7PF	106.90	107.07	107.08	107.07	107.0 8	107.0 7	106.90	––	––	116.79
8PF	106.90	107.07	107.08	107.07	107.0 7	107.0 8	107.07	106.90	––	116.78
9PF	106.90	107.07	107.08	107.07	107.0 8	107.0 7	107.08	107.07	106.90	116.76

*:, Intermediate bond distances between rings.

Table 6
Optimized bond angle of polypyrrole (n=1, 2, 3, 4, 5, 6, 7, 8, 9), using B3LYP/6-31G** level of theory (Atomic labels are with reference to Fig. 3).

Spe cies	I 1C-2NH-3C	II 1C-2NH-3C	III 1C-2NH-3C	IV 1C-2NH-3C	V 1C-2NH-3C	VI 1C-2NH- 3C	VII 1C-2NH-3C	VIII 1C-2NH-3C	IX 1C-2NH-3C	a...b...c*
1PPy	109.80	––	––	––	––	––	––	––	––	––
2PPy	110.23	110.2 3	––	––	––	––	––	––	––	121.51
3PPy	110.22	110.7 7	110.22	––	––	––	––	––	––	121.71
4PPy	110.20	110.6 3	110.63	110.20	––	––	––	––	––	121.63
5PPy	110.21	110.7 8	110.79	110.78	110.21	––	––	––	––	121.76
6PPy	110.19	110.6 4	110.76	110.77	110.77	110.21	––	––	––	121.80
7PPy	110.21	110.7 5	110.62	110.76	110.78	110.78	110.21	––	––	121.77
8PPy	110.21	110.7 7	110.75	110.63	110.75	110.77	110.77	110.21	––	121.61
9PPy	110.21	110.7 5	110.63	110.72	110.61	110.76	110.77	110.77	110.207 32	121.62
Exp.	11.82									

*:, an intermediate bond distances between rings. Exp.: experimental values.

Table 7
NBO and Mulliken charge distribution calculation of PPy, PF, PTh where n= 1....9 repeating units at B3LYP/6-31G (d, p) level of DFT.

# of Ring	Species	QMullikan	QNBO
I	1PF	1.338	2.264
	1PPy	1.482	2.727
	1PTh	1.445	2.93
II	2PF	0.03	0.122
	2PPy	0.602	0.15
	2PTh	0.105	0,745
III	3PF	4.556	6.422
	3PPy	5.368	7.196
	3PTh	3.351	6.788
IV	4PF	−0.027	0.884
	4PPy	0.0098	0.017
	4PTh	0.109	252.89
V	5PF	7.773	10.562
	5PPy	9.323	10.64
	5PTh	5.326	10.406
VI	6PF	−1.318	4.765
	6PPy	11.506	12.780
	6PTh	−0.195	452.40
VII	7PF	10.501	14.349
	7PPy	13.248	16.342
	7PTh	6.805	14.346
VIII	8PF	12.604	16.44
	8PPy	15.217	18.611
	8PTh	8.258	16.53
IX	9PF	14.21	19.376
	9PPy	16.838	20.882
	9PTh	9.195	-18.378

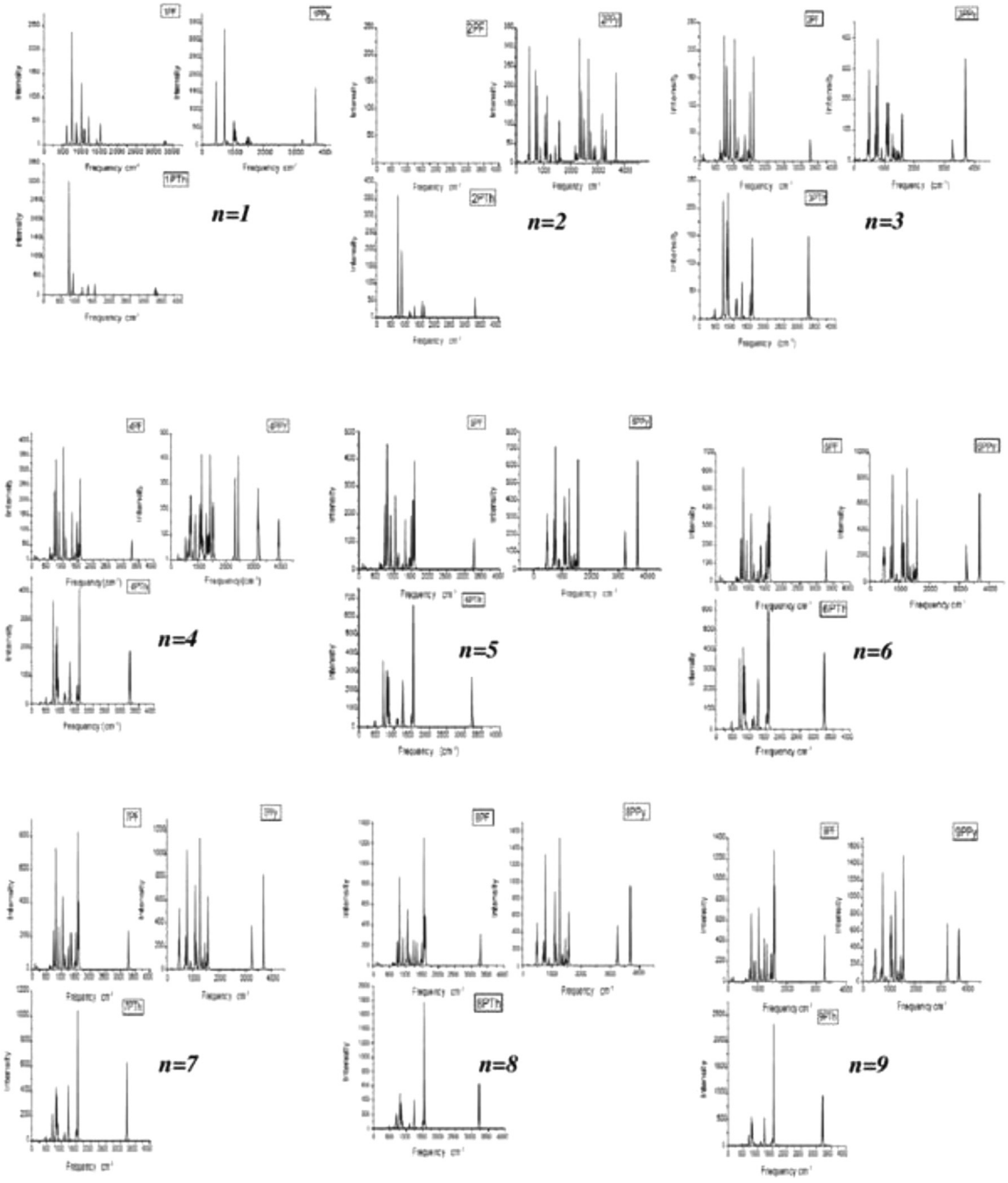

Fig. 5. Scaled Infrared spectrums of PF, PPy and PTh from n=1...9.

HOMO and LUMO diagram of PPy, PF and PTh are given in Figs. 6 and 7. The HOMO and LUMO of PPy (n=1.....9) are extended to all Carbons, hydrogen and nitrogen's (- NH-) and form a ladder like structure and involve delocalization over the entire molecule framework. Similarly for PF (n= 1.....9) are extended to all carbons and oxygen (-O-) and ladder like structure formed and involve delocalization over the entire molecule framework, while in PTh (n= 1... 9), the HOMO and LUMO are extended to all carbons and sulphur (-S-) and form a ladder like structure and involve delocalization over the entire molecule framework. The HOMO and LUMO energies and associated energy gap of the PPy, PF and PTh from monomers up to polymers repeating units are given in Table 12. The energy gap obtained from the difference between HOMO and LUMO. The HOMO, LUMO energy difference of PPy in the range of 3.44 eV, 2.78 eV for PF, while for PTh in the range of 2.49 eV. It can be concluded from the result that PTh show low energy gap as compared to PF and PPy. The low energy gap the more will be conductivity. So PTh is more conductive as compared to PF, PPy, and strongest candidates for forming material conductive. The conductivity range according to the calculated data is PTh > PF > PPy.

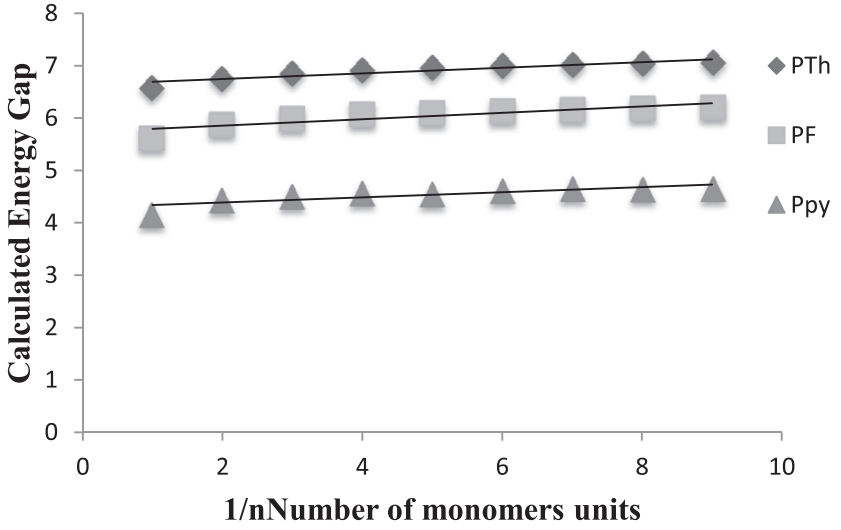

Fig. 6. Plot of the calculated Energy band gap ΔE of PTh, PF, PPy against the reciprocal of corresponding oligomers length, i.e, the number of monomers units.

Table 8
Calculated Excitation Energies, Oscillator Strengths, and Molecular Orbit- als (MOs) of the First Allowed Singlet Transition Involved in the Excitation for PF, Where n = 1…9 at B3LYP/6- 31G (d, p) Level of Theory.

Species	MOs	Energy (eV)	Wavelength (nm)	Oscillator Strength	Exp O.S
1PF	18→19	6.4988	190.78	0.1440	
2PF	*35→36*	*4.5646*	*271.62*	*0.5772*	
3PF	52→53	3.7052	334.62	0.8517	
4PF	*69→70*	*3.2304*	*383.81*	*1.2074*	1.30
5PF	86→87	2.9310	423.01	1.5309	1.66
6PF	*103→104*	*2.7287*	*454.37*	*1.8474*	2.00
7PF	120→121	2.5847	479.68	2.1474	2.32
8PF	137→138	2.4788	500.18	2.4434	
9PF	154→155	2.3992	516.78	2.7342	

Exp O.S: experimental values of oscillator strength

Table 9
Calculated Excitation Energies, Oscillator Strengths, and Molecular Orbital's (MOs) of the First Allowed Singlet Transition Involved in the Excitation for PPy, Where n = 1…9 at B3LYP/6- 31G (d, p) Level of Theory.

Species	MOs	Energy (eV)	Wavelength (nm)	Oscillator Strength
1PPy	18→19	6.7415	183.91	0.1439
2PPy	*35→36*	*4.8645*	*254.88*	*0.5512*
3PPY	52→53	4.1046	302.06	0.8492
4PPy	*69→70*	*3.6309*	*341.47*	*1.1963*
5PPy	86→87	3.3964	365.05	1.5015
6PPy	*103→104*	*3.2333*	*383.47*	*1.7975*
7PPy	120→121	3.1128	398.30	2.0856
8PPy	137→138	3.0319	408.93	2.3894
9PPy	154→155	2.9676	417.80	2.6879

Table 10
Calculated Excitation Energies, Oscillator Strengths, and Molecular Orbital's (MOs) of the First Allowed Singlet Transition Involved in the Excitation for PTh, Where n = 1…9 at B3LYP/6- 31G (d, p) Level of Theory.

Species	MOs	Energy (eV)	Wavelength (nm)	Oscillator Strength
1PTh	22→23	5.9207	209.41	0.0873
2PTh	*43→44*	*4.0235*	*308.15*	*0.4288*
3PTh	64→65	3.2643	379.82	0.8113
4PTh	*85→86*	*2.8353*	*437.29*	*1.2159*
5PTh	106→107	2.5677	482.86	1.6051
6PTh	*127→128*	*0.3812*	*520.67*	*1.9814*
7PTh	148→149	2.3136	535.88	2.3128
8PTh	169→170	2.2123	560.42	2.6563
9PTh	190→191	2.1358	580.50	2.9925

Table 11
Comparison of theoretically calculated IR intensities, Frequency, Mode number and vibrational assignment of PPy, PF and PTh (n= 1…9), using B3LYP/6- 31G (d, p) level of theory.

Ring #	Specie	Mode #	Frequency	IR Intensi- ty	Vibration
I	1PPy	1	461.26	77.43	γ.
	1PF	4	759.44	77.6380	Wagg
	1PTh	5	729.6	102.6	ν ^{as}, Def(ring)
II	2PPy	8	489.59	18.959	Γ
	2PF	11	733.75	72.1388	Γ
	2PTh	12	681.0	0.000	Wagg
III	3PPy	24	768.52	114.35	Wagg
	3PF	35	1042.00	10.1922	B
	3PTh	23	696.5	106.5	Γ
IV	4PPy	55	1105.01	119.5703	B
	4PF	29	799.36	105.412	Wagg
	4PTh	32	701.2	0.0000	Wagg, Def (ring)
V	5PPy	45	785.78	28.8778	Wagg
	5PF	61	1043.23	3.3831	B
	5PTh	38	688.3	0.0152	ν as
VI	6PPy	51	762.87	48.1890	Wagg
	6PF	50	810.49	0.0002	Γ
	6PTh	107	1547.9	339.5	ν ^{as}, Def (ring)
VII	7PPy	138	1562.25	0.8400	ν ^{as}, Def (ring)
	7PF	59	810.41	18.70	Γ
	7PTh	127	1572.02	0.6692	ν ^{as}, Def (ring)
VIII	8PPy	74	768.81	4.4737	Wagg
	8PF	141	1552.63	367.55	ν as
	8PTh	144	1555.0	1.235	ν as
IX	9PPy	78	762.60	48.0833	Wagg
	9PF	159	1553.53	504.88	ν as
	9PTh	163	1563.1	7.403	ν as

β: Scissoring, ν^{as}: Asymmetric stretching, Wagg: wagging, Def: ring deformation, γ: Twisting are predominated terms used/listed in the table.

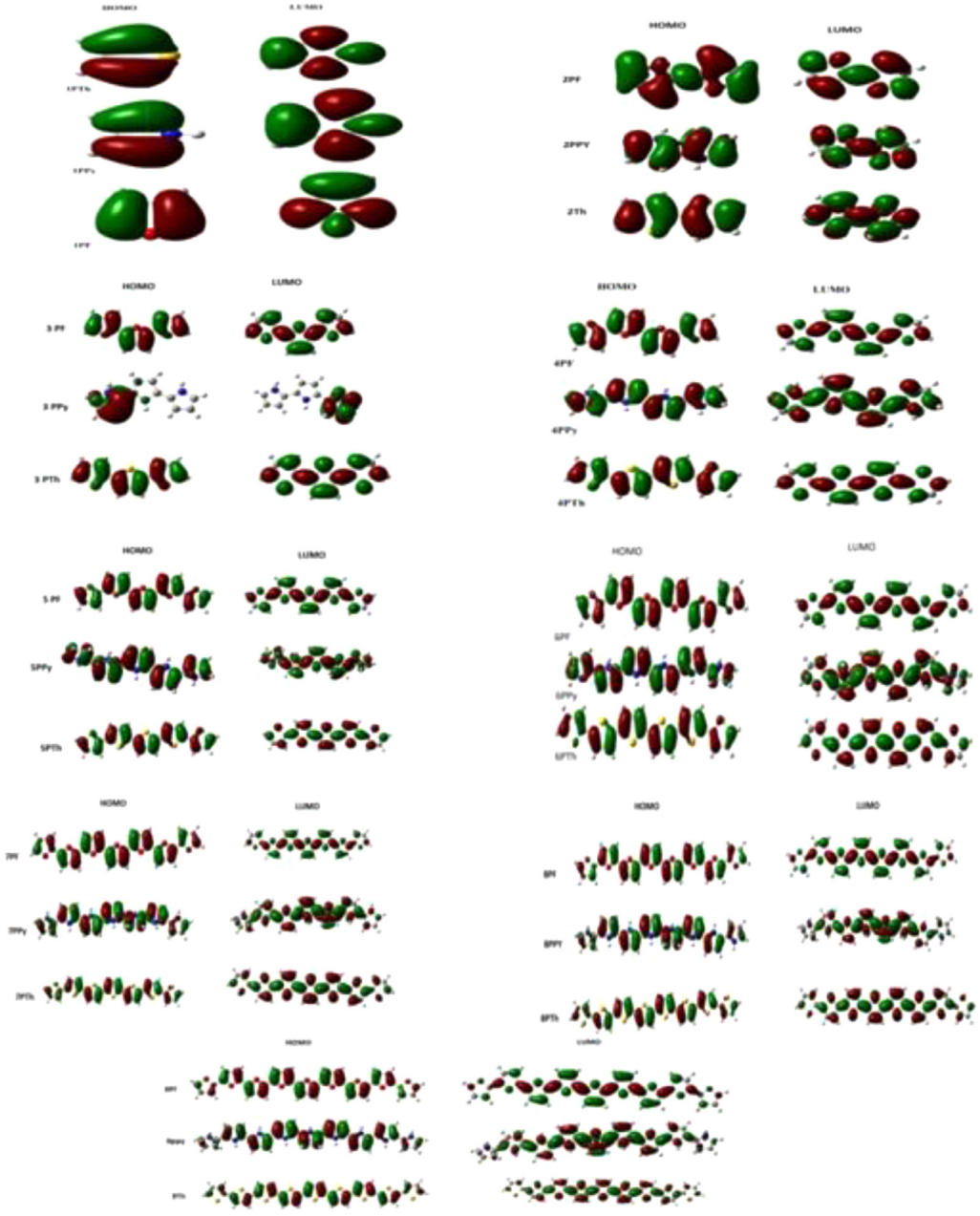

Fig. 7. Frontier molecular orbital of PPy, PF and PTh, where n=1...9.

Table 12
HOMO, LUMO and band gap calculation for PPy, PF, PTh where n= 1...9 at B3LYP/6-31G (d, p) level of DFT.

# Of Rings	Specie	LUMO e ^{V}	HOMO e^{V}	Energy gap(ΔE)
I	1PF	0.5053	6.1225	5.617
	1PPy	1.3461	5.5037	4.158
	1PTh	−0.2291	6.3486	6.577
II	2PF	−0.6122	5.2683	5.881
	2PPy	0.3232	4.7628	4.439
	2PTH	−1.2626	5.4863	6.749
III	3PF	−1.0707	4.9184	5.989
	3PPy	−0.0642	4.4444	4.509
	3PTh	−1.7007	5.1470	6.848
IV	4PF	−1.3181	4.7598	6.077
	4PPy	−0.3159	4.2553	4.571
	4PTh	−1.9439	4.9690	6.913
V	5PF	−1.4715	4.6286	6.100
	5PPy	−0.3828	4.1698	4.553
	5PTh	−2.0906	4.8702	6.960
VI	6PF	−1.5733	4.5609	6.134
	6PPy	−0.4998	4.1110	4.611
	6PTh	−2.1905	4.8052	6.996
VII	7PF	−1.6462	4.5162	6.162
	7PPy	−0.5605	4.0964	4.657
	7PTh	−2.2177	4.7987	7.016
VIII	8PF	−1.6996	4.4841	6.184
	8PPy	−0.6024	4.0430	4.645
	8PTh	−2.2716	4.7666	7.038
IX	9PF	−1.7401	4.4613	6.201
	9PPy	−0.6370	4.0218	4.659
	9PTh	−2.3124	4.7434	7.056

Exp*: PTh = 2.59 [45–48]
PF = 3.19 ([46]· [49])
PPy = 2.9 ([2]· [35]· [46])

4. Conclusions

DFT calculations were carried out for the purpose of comparative study of the electronic, structural and spectroscopic properties of the neutral heterocyclic polymers polypyrrole, polyfuran and polythiophene. Optimized geometric parameters were evaluated and it was observed that PTh show more/good interaction ability then PF and PPy as in the order PTh > PF >PPy. The net charge transfer in these polymers is simulated with NBO and Milliken charge analysis. NBO (QNBO) and Milliken (QMULLIKEN) charge analysis also go side by side with the result from optimized geometric parameters analysis. The UV-Vis spectra of PF, PTh, PPy from monomer to 9 repeated unit are simulated respectively. It is concluded that by increasing conjugation length the absorption also increases. Among PF, PTH, PPy the polythiophene show more absorption then PPy and PF. In vibrational analysis the band peak in the 1600–900 cm^{-1} region give information about the short and extended π conjugation length. The number of peaks in this region is evidence of the presence of conjugation in the polymeric backbone. The HOMO and LUMO energy differences observed for PTh is in the range of 2.44eV, for PF 2.78eV and for PPy [32] 3.44eV which predict PPy to be the strongest and PF to be the weakest candidate for forming conductive material through oxidative doping. On the other hand, PTh is found to have the greatest capacity for reductive doping followed by PF and PPy. From this primary work we conclude that the Frontier molecular orbital (HOMO and LUMO), band gap, UV–vis, IR, charge analysis and optimized polymeric geometry show consistency with each other and with available experimental data.

Author statement

All authors are contributed equally.

Declaration of Competing Interest

The authors declare that they have no known competing financial interests or personal relationships that could have appeared to influence the work reported in this paper.

Data availability

No data was used for the research described in the article.

References

[1] Z Soos, H. Keller, Comparison of columnar organic and inorganic solids, in: Chemistry and Physics of One-Dimensional Metals, Springer, 1977, pp. 391–412.
[2] M Senevirathne, A Nanayakkara, G. Senadeera, A theoretical investigation of band gaps of conducting polymers—polythiophene, polypyrrole and polyfuran, Proc. Tech. Sessions 23 (2007) 47–53.
[3] SC. Rasmussen, The path to conductive polyacetylene, Bull. Hist. Chem. 39 (1) (2014) 64–72.
[4] G Sonmez, H Meng, Q Zhang, F. Wudl, A highly stable, new electrochromic polymer: poly (1, 4-bis (2-(3′, 4′-ethylenedioxy) thienyl)-2-methoxy-5-2 ″-ethylhexyloxybenzene), Adv. Funct. Mater. 13 (9) (2003) 726–731.
[5] J Stejskal, I Sapurina, M. Trchová, Polyaniline nanostructures and the role of aniline oligomers in their formation, Progr. Polym. Sci. 35 (12) (2010) 1420–1481.
[6] W. Little, Possibility of synthesizing an organic superconductor, Phys. Rev. 134 (6A) (1964) A1416.
[7] F Benvenuti, AMR Galletti, C Carlini, G Sbrana, A Nannini, P. Bruschi, Synthesis, structural characterization and electrical properties of highly conjugated soluble poly (furan) s, Polymer 38 (19) (1997) 4973–4982.
[8] M González-Tejera, ES de la Blanca, I. Carrillo, Polyfuran conducting polymers: Synthesis, properties, and applications, Synth. Met. 158 (5) (2008) 165–189.
[9] R Kumar, S Singh, B. Yadav, Conducting polymers: synthesis, properties and applications, Int. Adv. Res. J. Sci., Eng. Technol. 2 (11) (2015) 110–124.
[10] Y Abbas, A. Abbas, Dielectric and gas sensing properties of in situ electrochemically polymerized PPy-MgO-WO3 nanocomposite films, Iraqi J. Sci. 62 (2021) 2915–2933.
[11] N Joy, J Eldho, R. Francis, Conducting polymers: an introduction, Biomed. Appl. Polym. Mater. Compos. (2016) 21–35.
[12] M. Ates, Review study of electrochemical impedance spectroscopy and equivalent electrical circuits of conducting polymers on carbon surfaces, Progr. Org. Coat. 71 (1) (2011) 1–10.
[13] S Okur, U. Salzner, Theoretical modeling of the doping process in polypyrrole by calculating UV/vis absorption spectra of neutral and charged oligomers, J. Phys. Chem. A 113 (31) (2009) 9050.
[14] Charef F. Matériau d'électrode à base du carbone modifié par un film de polymère et contenant du bioxyde de Manganèse 2018.
[15] US Schubert, A Winter, GR. Newkome, Electropolymerization—an item-centered view on ruthenopolymers, in: Ruthenium-Containing Polymers, Springer, 2021, pp. 187–274.
[16] M Ates, T Karazehir, A Sezai Sarac, Conducting polymers and their applications, Curr. Phys. Chem. 2 (3) (2012) 224–240.
[17] H-K Jun, Y-S Hoh, B-S Lee, S-T Lee, J-O Lim, D-D Lee, et al., Electrical properties of polypyrrole gas sensors fabricated under various pretreatment conditions, Sens. Actuat. B: Chem. 96 (3) (2003) 576–581.
[18] S Biswas, LT. Drzal, Multilayered nanoarchitecture of graphene nanosheets and polypyrrole nanowires for high performance supercapacitor electrodes, Chem. Mater. 22 (20) (2010) 5667–5671.
[19] Y Huang, Y Wang, G Sang, E Zhou, L Huo, Y Liu, et al., Polythiophene derivative with the simplest conjugated-side-chain of alkenyl: synthesis and applications in polymer solar cells and field-effect transistors, J. Phys. Chem. B 112 (43) (2008) 13476–13482.
[20] F Li, M Cao, Y Feng, R Liang, X Fu, M. Zhong, Site-specifically initiated controlled/living branching radical polymerization: a synthetic route toward hierarchically branched architectures, J. Am. Chem. Soc. 141 (2) (2018) 794–799.
[21] JM Pringle, M Forsyth, DR MacFarlane, K Wagner, SB Hall, Officer DL. The influence of the monomer and the ionic liquid on the electrochemical preparation of polythiophene, Polymer 46 (7) (2005) 2047–2058.
[22] B Amna, HM Siddiqi, A Hassan, T. Ozturk, Recent developments in the synthesis of regioregular thiophene-based conjugated polymers for electronic and optoelectronic applications using nickel and palladium-based catalytic systems, RSC Adv. 10 (8) (2020) 4322–4396.
[23] M Nicho, H Hu, C López-Mata, J. Escalante, Synthesis of derivatives of polythiophene and their application in an electrochromic device, Sol. Energy Mater. Sol. Cells 82 (1-2) (2004) 105–118.
[24] G Dos Reis, I Dias, H De Santana, J Duarte, E Laureto, E Di Mauro, et al., Analysis of optical properties of poly (3-methylthiophene)(P3MT) electrochemically synthesized, Synth. Met. 161 (3-4) (2011) 340–347.
[25] S Jadoun, U. Riaz, A review on the chemical and electrochemical copolymerization of conducting monomers: recent advancements and future prospects, Polym.-Plast. Technol. Mater. 59 (5) (2020) 484–504.
[26] SK Mal, S Some, JK. Ray, Heteroaryl radicals: a furyl radical in the synthesis of the tricyclic framework of eremophilane sesquiterpenoids, Synlett 2005 (12) (2005) 1951–1953.

[27] T Aoai, R Nishio, N Hayashi, K. Nomura, Photo doping process of conductive polymer with PAG and application for organic thermoelectric materials, J. Photopolym. Sci. Technol. 29 (2) (2016) 335–341.
[28] S-C Qi, J-i Hayashi, L. Zhang, Recent application of calculations of metal complexes based on density functional theory, RSC Adv. 6 (81) (2016) 77375–77395.
[29] N Arshad, AK Singh, B Chugh, M Akram, F Perveen, I Rasheed, et al., Experimental, theoretical, and surface study for corrosion inhibition of mild steel in 1 M HCl by using synthetic anti-biotic derivatives, Ionics 25 (10) (2019) 5057–5075.
[30] I Czekaj, N. Sobuś, Concepts of modern technologies of obtaining valuable biomass-derived chemicals, Tech. Trans. 115 (8) (2018) 35–58.
[31] H Ullah, A-u-HA Shah, S Bilal, K. Ayub, DFT study of polyaniline NH3, CO2, and CO gas sensors: comparison with recent experimental data, J. Phys. Chem. C 117 (45) (2013) 23701–23711.
[32] J Ma, S Li, Y. Jiang, A time-dependent DFT study on band gaps and effective conjugation lengths of polyacetylene, polyphenylene, polypentafulvene, polycyclopentadiene, polypyrrole, polyfuran, polysilole, polyphosphole, and polythiophene, Macromolecules 35 (3) (2002) 1109–1115.
[33] C Liang, Y Wang, D Li, X Ji, F Zhang, Z He, Modeling and simulation of bulk heterojunction polymer solar cells, Sol. Energy Mater. Sol. Cells 127 (2014) 67–86.
[34] H Cao, J Ma, G Zhang, Y. Jiang, Borole/thiophene cooligomers and copolymers with quinoid structures and biradical characters, Macromolecules 38 (4) (2005) 1123–1130.
[35] S Glenis, M Benz, E LeGoff, J Schindler, C Kannewurf, M. Kanatzidis, Polyfuran: a new synthetic approach and electronic properties, J. Am. Chem. Soc. 115 (26) (1993) 12519–12525.
[36] D Svatunek, T Hansen, KN Houk, TA. Hamlin, How the Lewis base F–catalyzes the 1, 3-dipolar cycloaddition between carbon dioxide and nitrilimines, J. Org. Chem. 86 (5) (2021) 4320–4325.
[37] B Han, CM Isborn, L. Shi, Determining partial atomic charges for liquid water: assessing electronic structure and charge models, J. Chem. Theory Comput. 17 (2) (2021) 889–901.
[38] H Ullah, A-u-HA Shah, S Bilal, K. Ayub, Doping and dedoping processes of polypyrrole: DFT study with hybrid functionals, J. Phys. Chem. C 118 (31) (2014) 17819–17830.
[39] SK Adjokatse, AK Mishra, UV. Waghmare, Dielectric and piezoelectric responses of nylon-7: a first-principles study, Polymer 53 (13) (2012) 2751–2757.
[40] H Sun, Z Hu, C Zhong, S Zhang, Z. Sun, Quantitative estimation of exciton binding energy of polythiophene-derived polymers using polarizable continuum model tuned range-separated density functional, J. Phys. Chem. C 120 (15) (2016) 8048–8055.
[41] M.E. Foster, B.M. Wong, Nonempirically tuned range-separated DFT accurately predicts both fundamental and excitation gaps in DNA and RNA nucleobases, J. Chem. Theory Comput. 8 (8) (2012) 2682–2687.
[42] M. Kurban, B. Gündüz, F. Göktaş, Experimental and theoretical studies of the structural, electronic and optical properties of BCzVB organic material, Optik 182 (2019) 611–617.
[43] B. Gündüz, M. Kurban, Photonic, spectroscopic properties and electronic structure of PTCDI-C8 organic nanostructure, Vibr. Spectrosc. 96 (2018) 46–51.
[44] M. Kurban, T.R. Sertbakan, B. Gündüz, A combined experimental and DFT/TD-DFT studies on the electronic structure, structural and optical properties of quinoline derivatives, J. Mol. Model. 26 (6) (2020) 1–7.
[45] T-C Chung, J Kaufman, A Heeger, F. Wudl, Charge storage in doped poly (thiophene): optical and electrochemical studies, Phys. Rev. B 30 (2) (1984) 702.
[46] J Mintmire, C White, M. Elert, Conformation and electronic structure of heterocyclic ring chain polymers, Synth. Met. 25 (2) (1988) 109–119.
[47] A Bakhshi, J Ladik, M. Seel, Comparative study of the electronic structure and conduction properties of polypyrrole, polythiophene, and polyfuran and their copolymers, Phys. Rev. B 35 (2) (1987) 704.
[48] K Kaeriyama, S Tanaka, M-A Sato, K. Hamada, Structure and properties of polythiophene derivatives, Synth. Met. 28 (1-2) (1989) 611–620.
[49] A Breeze, Z Schlesinger, S Carter, P. Brock, Charge transport in TiO 2/M E H− P P V polymer photovoltaics, Phys. Rev. B 64 (12) (2001) 125205.